Supporting Information

Table of Contents

1. Experimental section

1.1 Synthetic route of DOX-BOD

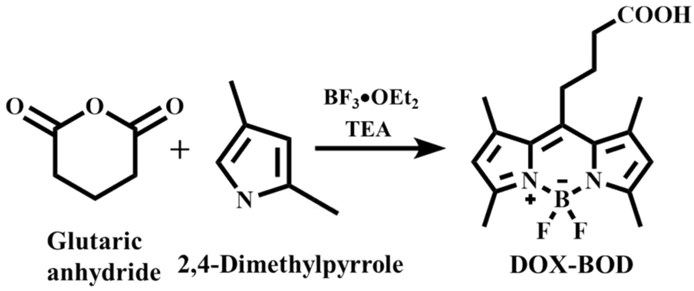

Scheme S1. Synthetic route of DOX-BOD

1.2 Fluorescence measurement

DMSO was used to prepare 1 mM stock solution. A mixture of 1.98 mL of PBS buffer (10 mM, pH 7.3) and 0.02 mL of DOX-BOD@ZIF-8 stock solution was prepared in a centrifuge tube. The maximum absorption wavelength was measured by microplate reader (Readmax 1900). After the maximum absorption wavelength was obtained, fluorescent spectrophotometer (F97Pro) was used to measure the maximum emission wavelength.

2. Relative absorption and fluorescence spectrum of DOX-BOD@ZIF-8

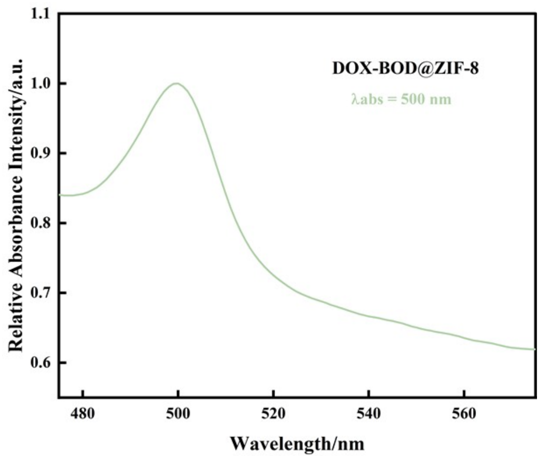

Fig. S1. Relative absorption spectrum of DOX-BOD@ZIF-8 (10 μM) in PBS buffer (10 mM, pH 7.3, containing less than 1% DMSO) at room temperature, and the maximum absorbance at 500 nm was normalized to 1.

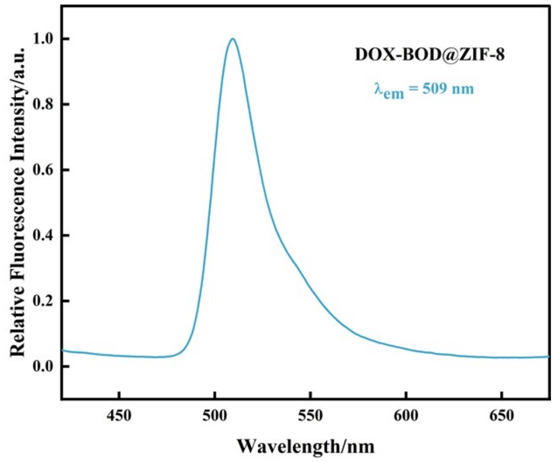

Fig. S2. Relative fluorescence spectrum of DOX-BOD@ZIF-8 (10 μM) in PBS buffer (10 mM, pH 7.3, containing less than 1% DMSO) at room temperature, and the maximum fluorescence intensity at 509 nm was normalized to 1, λ_{ex} = 358 nm.

3. Determination of encapsulation efficiency

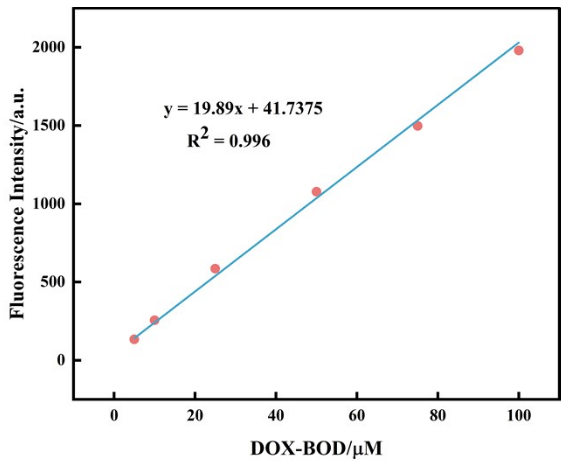

Fig. S3. Standard curve of DOX-BOD from fluorescence spectra.

The encapsulation efficiency of DOX-BOD@ZIF8 was investigated by fluorescence spectroscopy. The fluorescence intensity of DOX-BOD was determined using a specific concentration gradient and a standard curve was constructed. During the synthesis of DOX-BOD @ ZIF-8, all supernatants were collected and dispersed uniformly by ultrasound. The fluorescence intensity was measured at an excitation wavelength of 358 nm. According to the standard curve of DOX-BOD, the concentration of DOX-BOD@ZIF-8 sample was obtained and the encapsulation rate was calculated to be 36.776%.

4. pH stability of DOX-BOD

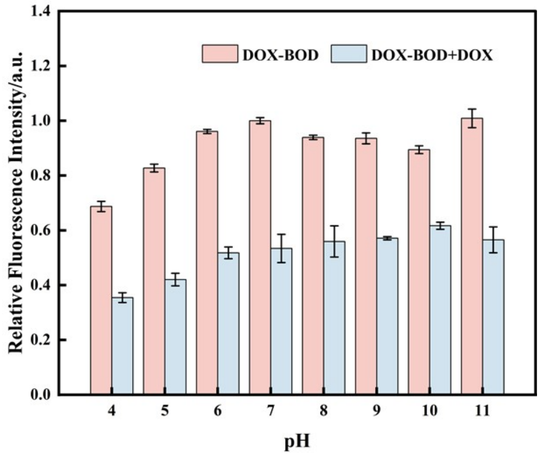

Fig. S4. Relative fluorescence intensity of DOX-BOD (20 μM) in different pH PBS buffer (10 mM) before and after mixed with DOX (100 μM), and the maximum fluorescence intensity at pH 7 was normalized to 1.

5. Fluorescence spectra of DOX-BOD in different concentrations of DOX

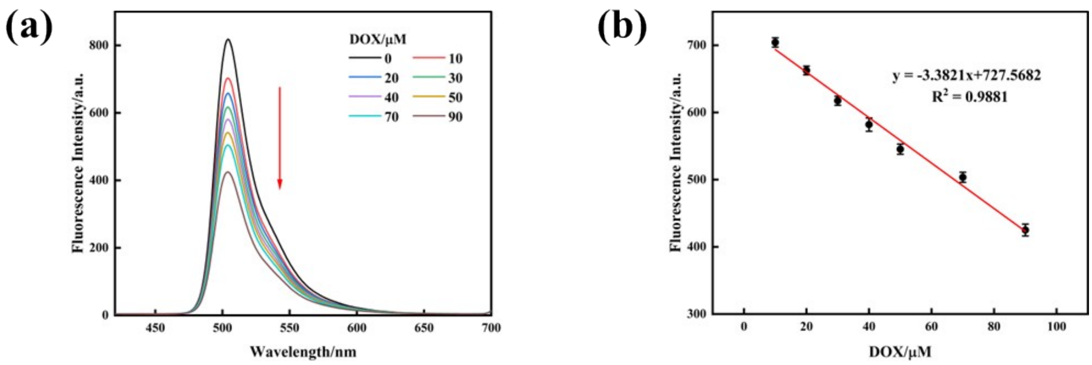

Fig. S5. The titration test of DOX-BOD. (a) Fluorescence spectra of DOX-BOD (20 μM) mixed with different concentrations of DOX (0, 10, 20, 30, 40, 50, 70, 90 μM) in PBS buffer (10 mM, pH 7.3), and the mixed solution was reacted at room temperature for 5 min. (b) Fitting plot of (a).

6. Absorption Spectra of DOX

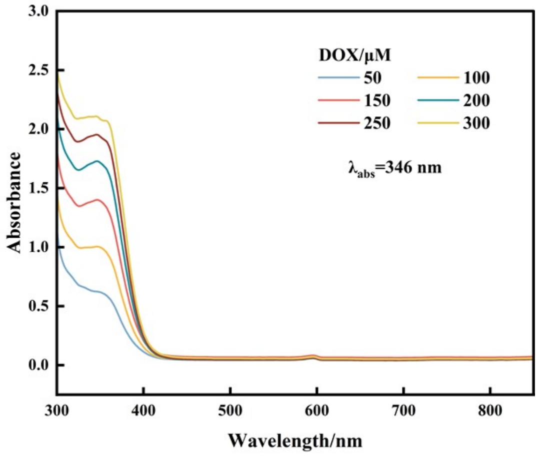

Fig. S6. Absorption spectra of DOX (50, 100, 150, 200, 250, 300 μM) in PBS buffer (10 mM, pH 7.3) at room temperature.

7. Fluorescence spectra of DOX

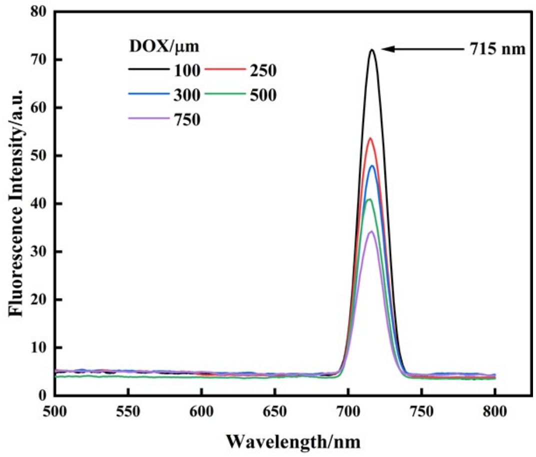

Fig.S7. Fluorescence spectra of DOX (from 100 to 750 μM, PBS buffer 10 mM, pH 7.3, λex = 358 nm, room temperature, the 300 μL of the DOX solution was transferred to a slit cuvette and set on a fluorescence spectrophotometer (F97Pro, Shanghai Lengguang) to get the fluorescence spectrum).

8. Comparison of different methods for detection of DOX

Table S1. Comparison of several testing methods of DOX.

Analytical Method	Dynamic range (μM)	DOX (LOD) (μM)
electrochemistry[1]	0.50-1000	0.14
Thin-layer chromatography[2]	2.25-22.5	0.14
flow injection analysis[3]	11.2-562.5	3.38
high performance liquid chromatography[4]	0.02-0.9	8×10^{-3}
capillary electrophoresis[5]	2.25-450	0.18
DOX-BOD@ZIF-8	10-100	2.72

9. Comparison of different fluorescent materials for the detection of DOX

Table S2. Comparison of the fluorescent materials that have been reported for the detection of DOX.

Probe	Dynamic range (μM)	DOX (LOD) (μM)
NCQDs[6]	5-50	87×10^{-3}
S dots/Ca^{2+} [7]	0.5-25	0.19
BSA-AuNCs[8]	2-30	36×10^{-3}
TGA/CdTe QDs[9]	1.9-61	0.11
CDs@MOF(Eu))[10]	0-60	360
CuNCs@OVA[11]	1-1000	0.27

10. Characterization spectra[12]

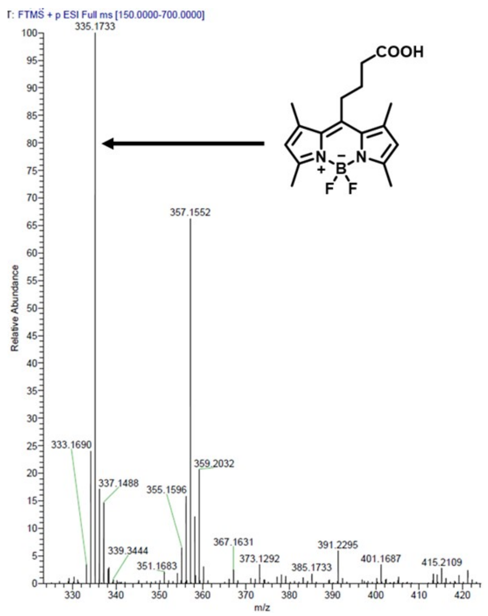

Fig. S8. HRMS analysis of DOX-BOD

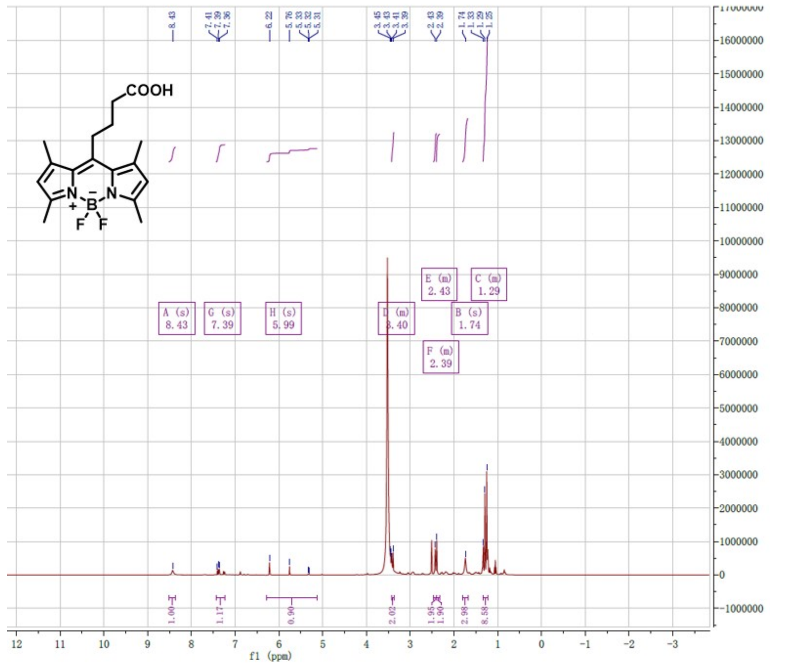

Fig. S9. ^{1}H NMR spectrum of DOX-BOD (DMSO-d_6, 400 MHz)

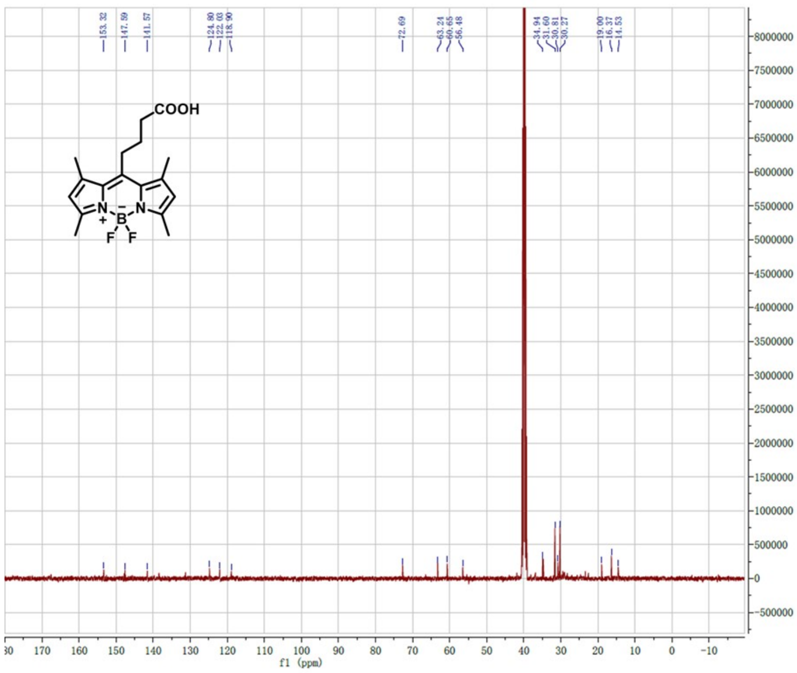

Fig. S10. ^{13}C NMR spectrum of DOX-BOD (DMSO-d_6, 101 MHz)

References

1. Cui, Z.; Guo, S.; Yan, J.; Li, F.; He, W., BiOBr nanosheets with oxygen vacancies and lattice strain for enhanced photoelectrochemical sensing of doxycycline. *Appl. Surf. Sci.*, **2020,** *512*, 145695, doi.org/10.1016/j.apsusc.2020.145695.

2. Mohammad, M.; Zawilla, N., Thin-layer and column-chromatographic methods for simultaneous analysis of ambroxol hydrochloride and doxycycline hyclate in a binary mixture. *J. Planar Chromatogr.-Mod. TLC*, **2009,** *22* (3), 201-206, doi.org/10.1556/jpc.22.2009.3.8.

3. Palamy, S.; Ruengsitagoon, W., A novel flow injection spectrophotometric method using plant extracts as green reagent for the determination of doxycycline. *Spectrochim. Acta, Part A*, **2017,** *171*, 200-206, doi.org/10.1016/j.saa.2016.08.011.

4. Dil, E. A.; Ghaedi, M.; Asfaram, A.; Tayebi, L.; Mehrabi, F., A ferrofluidic hydrophobic deep eutectic solvent for the extraction of doxycycline from urine, blood plasma and milk samples prior to its determination by high-performance liquid chromatography-ultraviolet. *J. Chromatogr. A*, **2020,** *1613*, 460695, doi.org/10.1016/j.chroma.2019.460695.

5. Mu, G.; Liu, H.; Xu, L.; Tian, L.; Luan, F., Matrix Solid-Phase Dispersion Extraction and Capillary Electrophoresis Determination of Tetracycline Residues in Milk. *Food Anal. Meth.*, **2011,** *5* (1), 148-153, doi.org/10.1007/s12161-011-9225-1.

6. Feng, X., Ashley, J., Zhou, T., & Sun, Y., Fluorometric determination of doxycycline based on the use of carbon quantum dots incorporated into a molecularly imprinted polymer. *Microchim. Acta*, **2018**, *185* (11), 500. doi:10.1007/s00604-018-2999-8.

7. Zhuang, Y., Lin, B., Yu, Y., Wang, Y., Zhang, L., Cao, Y., & Guo, M., A ratiometric fluorescent probe based on sulfur quantum dots and calcium ion for sensitive and visual detection of doxycycline in food. *Food Chem.*, **2021**, *356*, 129720. doi:10.1016/j.foodchem.2021.129720.

8. Ding, L., Zhao, Y., Li, H., Zhang, Q., Yang, W., Fu, B., & Pan, Q., A highly selective ratiometric fluorescent probe for doxycycline based on the sensitization effect of bovine serum albumin. *J. Hazard. Mater.*, **2021**, *416*, 125759. doi:10.1016/j.jhazmat.2021.125759.

9. Tashkhourian, J., Absalan, G., Jafari, M., & Zare, S., A rapid and sensitive assay for determination of doxycycline using thioglycolic acid-capped cadmium telluride quantum dots. *Spectrochim. Acta, Part A*, **2016**, *152*, 119-125. doi:10.1016/j.saa.2015.07.063.

10. Fu, X., Lv, R., Su, J., Li, H., Yang, B., Gu, W., & Liu, X., A dual-emission nano-rod MOF equipped with carbon dots for visual detection of doxycycline and sensitive sensing of MnO4. *RSC Adv.*, **2018**, *8* (9), 4766-4772. doi:10.1039/c7ra12252g.

11. Yang, K., Wang, Y., Lu, C., & Yang, X., Ovalbumin-directed synthesis of fluorescent copper nanoclusters for sensing both vitamin B-1 and doxycycline. *J. Lumin.*, **2018**, *196*, 181-186. doi:10.1016/j.jlumin.2017.12.038.

12. Ding, L. Z.; Guo, Q.; Sun, X. L.; Hu, G. W.; Hu, J. H.; Fan, S. W.; Fu, Y. Q., Synthesis and Performance Testing of a BODIPY Fluorescent Probe for the Detection of Doxycycline Residues in Water Environment. *ChemistrySelect*, **2022,** *7* (40), e202203410, doi.org/10.1002/slct.202203410.